Signal Transduction:

Modulation of Endoplasmic Reticulum Ca^{2+} Store Filling by Cyclic ADP-ribose Promotes Inositol Trisphosphate (IP_3)-evoked Ca^{2+} Signals

Michiko Yamasaki-Mann, Angelo Demuro and Ian Parker

J. Biol. Chem. 2010, 285:25053-25061.
doi: 10.1074/jbc.M109.095257 originally published online June 10, 2010

THE JOURNAL OF BIOLOGICAL CHEMISTRY VOL. 285, NO. 32, pp. 25053–25061, August 6, 2010

Modulation of Endoplasmic Reticulum Ca^{2+} Store Filling by Cyclic ADP-ribose Promotes Inositol Trisphosphate (IP_3)-evoked Ca^{2+} Signals*

Received for publication, December 15, 2009, and in revised form, June 3, 2010 Published, JBC Papers in Press, June 10, 2010, DOI 10.1074/jbc.M109.095257

Michiko Yamasaki-Mann[‡1], **Angelo Demuro**[‡], **and Ian Parker**[‡§]

From the Departments of [‡]*Neurobiology and Behavior, and* [§]*Physiology and Biophysics, University of California, Irvine, California 92697*

In addition to its well established function in activating Ca^{2+} release from the endoplasmic reticulum (ER) through ryanodine receptors (RyR), the second messenger cyclic ADP-ribose (cADPR) also accelerates the activity of SERCA pumps, which sequester Ca^{2+} into the ER. Here, we demonstrate a potential physiological role for cADPR in modulating cellular Ca^{2+} signals via changes in ER Ca^{2+} store content, by imaging Ca^{2+} liberation through inositol trisphosphate receptors (IP_3R) in *Xenopus* oocytes, which lack RyR. Oocytes were injected with the non-metabolizable analog 3-deaza-cADPR, and cytosolic [Ca^{2+}] was transiently elevated by applying voltage-clamp pulses to induce Ca^{2+} influx through expressed plasmalemmal nicotinic channels. We observed a subsequent potentiation of global Ca^{2+} signals evoked by strong photorelease of IP_3, and increased numbers of local Ca^{2+} puffs evoked by weaker photorelease. These effects were not evident with cADPR alone or following cytosolic Ca^{2+} elevation alone, indicating that they did not arise through direct actions of cADPR or Ca^{2+} on the IP_3R, but likely resulted from enhanced ER store filling. Moreover, the appearance of a new population of puffs with longer latencies, prolonged durations, and attenuated amplitudes suggests that luminal ER Ca^{2+} may modulate IP_3R function, in addition to simply determining the size of the available store and the electrochemical driving force for release.

Elevations of cytosolic free Ca^{2+} are utilized as a ubiquitous cellular signaling mechanism to control diverse functions in virtually all cells of the body. The endoplasmic reticulum (ER)[2] forms one of the major Ca^{2+} stores, from which Ca^{2+} ions are liberated passively down their electrochemical gradient through the opening of Ca^{2+} release channels in the ER membrane including inositol trisphosphate receptors (IP_3R) and ryanodine receptors (RyR). Much attention has focused on these Ca^{2+} release channels, as they give rise to the dynamic and localized spatio-temporal patterns of Ca^{2+} signals that ensure appropriate control of functions ranging from secretion and electrical excitability to gene expression (1). Conversely, the energy-requiring processes, such as the sarco/endoplasmic reticulum calcium (SERCA) pump that sequesters Ca^{2+} ions back into the ER, have largely been regarded as important only for long-term Ca^{2+} homeostasis. However, increasing evidence indicates that sequestration mechanisms are also subject to dynamic regulation, which may both modulate the rates of cytosolic Ca^{2+} clearance, and determine the store of ER Ca^{2+} available for subsequent release (2–5).

In addition to simply determining the size of the available store and the electrochemical driving force for release, the luminal free Ca^{2+} concentration in the ER may functionally modulate the gating properties of Ca^{2+} release channels. The evidence is strongest for RyR, where it is well established that elevations of Ca^{2+} content in the sarcoplasmic reticulum of muscle enhance global Ca^{2+} release through RyRs (6). This arises thorough an increased in channel open probability (7–9), likely mediated via luminal Ca^{2+} sensing proteins such as calsequestrin (7). Similarly, IP_3-evoked Ca^{2+} signals are regulated by the ER luminal Ca^{2+} (10–13). However, although the existence of luminal Ca^{2+} binding site, or luminal Ca^{2+} sensing protein on luminal side of the IP_3R has been implicated (14, 15), little is known about how luminal Ca^{2+} may affect IP_3R function in intact cells.

Studies to examine the influence of luminal ER Ca^{2+} on IP_3R-mediated Ca^{2+} signaling in intact cells are complicated in cell types that also express RyRs, given that both channel types are themselves activated by cytosolic Ca^{2+} and may thus interact through Ca^{2+}-induced Ca^{2+} release (CICR). *Xenopus* oocytes, which lack RyRs (16), have thus been a favored model cell system in which to study Ca^{2+} signaling processes independent of RyR. In this system we had previously demonstrated that the second messenger cyclic ADP-ribose (cADPR) accelerates cytosolic Ca^{2+} clearance by enhancing SERCA activity (17), distinct from its well known action to promote Ca^{2+} liberation through RyR (18, 19).

In the present study, we again employed *Xenopus* oocytes to investigate whether cADPR-mediated enhancement of Ca^{2+} sequestration into the ER may play a physiological role in potentiating IP_3-evoked Ca^{2+} signals. Oocytes were injected with a non-metabolizable analog of cADPR, 3-deaza-cADPR, and Ca^{2+} sequestration was further enhanced by transiently elevating cytosolic [Ca^{2+}] by applying hyperpolarizing voltage pulses to induce Ca^{2+} influx through nicotinic channels expressed in the oocyte membrane. In combination, 3-deaza-cADPR and Ca^{2+} influx enhanced global cellular Ca^{2+} signals

* This work was supported, in whole or in part, by Grant GM48071 (to I. P.) from the National Institutes of Health.

[1] To whom correspondence should be addressed: Dept. of Neurology, David Geffen School of Medicine, University of California, Los Angeles, 635 Charles Young Dr. South, Los Angeles, CA 90095-7335. Tel.: 310-206-1966; Fax: 310-206-6906; E-mail: michikomann@ucla.edu.

[2] The abbreviations used are: ER, endoplasmic reticulum; IP_3R, inositol trisphosphate receptor; RyR, ryanodine receptors; cADPR, cyclic ADP-ribose; nAChR, nicotinic acetylcholine receptor; FDHM, half-maximal fluorescence amplitude.

elicited by subsequent photorelease of IP_3 after cytosolic Ca^{2+} had returned to basal levels. This effect was not evident with cADPR alone or following cytosolic Ca^{2+} elevation alone, indicating that the enhanced IP_3 response did not arise through direct actions of cADPR or Ca^{2+} on IP_3R, but likely resulted from enhanced ER store filling. Moreover, we observed changes in the kinetics, frequency, and amplitude of the local Ca^{2+} puffs that arise through concerted openings of small clusters of IP_3R, suggesting that luminal ER Ca^{2+} may modulate IP_3R function in addition to setting the electrochemical gradient that passively determines Ca^{2+} release.

EXPERIMENTAL PROCEDURES

Oocyte Preparation—Oocytes were removed via multiple surgeries on *Xenopus laevis* (purchased from Nasco International, Fort Atkinson, WI) according to the protocols approved by the UC Irvine Institutional Animal Care and Use committee, and stage V-VI oocytes were isolated after removing ovaries. Oocytes were treated with collagenase (1 mg/ml of collagenase type A1 for 30 min) to remove enveloping cell layers and were stored in modified Barth's solution (mM: NaCl, 88; KCl, 1; $NaHCO_3$, 2.4; $MgSO_4$, 0.82; $Ca(NO_3)2$, 0.33; $CaCl_2$, 0.41;Hepes, 5; gentamicin, 1 mg/ml; pH 7.4) for 1–5 days before use.

Expression of nAChRs—Plasmids containing cDNA clones coding for the muscle nicotinic acetylcholine receptor (nAChR) α, β, γ, δ subunits were linearized and transcribed *in vitro* with SP6 or T3 RNA polymerases, and corresponding cRNAs (molar ratio 2:1:1:1) were mixed to a final concentration of 0.1–1 mg/ml and injected (50 nl) into oocytes. Oocytes were maintained at 16 °C for 1–3 days to express nAChRs in the plasma membrane. Expression level was monitored using a voltage clamp to measure current in response to 100–500 nM ACh: oocytes showing currents >1 nA at −80 mV were selected for experiments.

Ca^{2+} Imaging and Photolysis of Caged IP_3—About 1 h before use, oocytes were injected with a solution containing Fluo-4 dextran, caged IP_3 (D-myo-inositol 1,4,5-trisphosphate $P^{4(5)}$-[1-(2-nitrophenyl)ethyl]ester and EGTA to give respective final intracellular concentrations of 40, 8, and 300 μM (assuming homogeneous distribution throughout a cytosolic volume of 1 μl). In some instances, 3-deaza-cADPR (0.8 μM final cytosolic concentration) was further included in the injection solution. After placing in the recording chamber, oocytes were voltage-clamped using a conventional two microelectrode technique. The membrane potential was held at 0 mV during superfusion with non-desensitizing concentration of ACh (100–500 nM) in Ringer's solution (mM: NaCl2, 120; KCl, 2; $CaCl_2$, 1.8; HEPES, 5; pH 7.4) and was briefly stepped to −120 mV to strongly increase the electrical driving force for Ca^{2+} influx (17, 20). Oocytes were imaged at room temperature by wide-field fluorescence microscopy using an Olympus inverted microscope (IX 71) equipped with a 40× oil-immersion objective, a 488-nm argon-ion laser for fluorescence excitation and a ccd camera (Cascade 128+: Roper Scientific) for imaging fluorescence emission (510–600 nm) at frame rates of 50 s^{-1}. Fluorescence was imaged within a 40 × 40 μm region within the animal hemisphere of the oocyte and measurements are expressed as a ratio ($\Delta F/F_o$) of the mean change in fluorescence at a given region of interest (ΔF) relative to the resting fluorescence at that region before stimulation (F_o). Mean values of F_o were obtained by averaging over several frames before stimulation. MetaMorph (Molecular Devices) was used for image processing, and measurements were exported to Microcal Origin version 6.0 (OriginLab, Northampton, MA) for analysis and graphing. Data are expressed as mean + 1 S.E., and significance was assessed by *t*-tests comparing before and after elevation of ER luminal Ca^{2+}.

Reagent—Fluo 4 dextran, high affinity (K_d: ~350 nM), and caged-$InsP_3$ were purchased from Invitrogen (Carlsbad, CA). 3-Deaza-cADPR and collagenase type A were from Sigma-Aldrich, and 8-Br-cADPR (IC_{50}: ~1 μM) was from BIOMOL International, L.P. (Plymouth Meeting, PA).

RESULTS

Cytosolic Ca^{2+} Elevation and cADPR Together Potentiate IP_3-evoked Global Ca^{2+} Signals—We had previously shown that 3-deaza-cADPR enhances the rate at which SERCA pump activity sequesters cytosolic Ca^{2+} in *Xenopus* oocytes; a cell type that lacks endogenous RyRs (17). Here we examined whether this may lead to an overfilling of ER Ca^{2+} stores that would be evident as an enhancement of subsequent Ca^{2+} liberation through IP_3R.

Fig. 1*A* shows a schematic of the experimental design. Recordings were made from oocytes that were injected a few days before use with mRNAs encoding the subunits of the muscle nAChR, so that Ca^{2+} influx through nAChR expressed in the plasma membrane could be used as a switch to transiently elevate cytosolic [Ca^{2+}] (17, 21). Oocytes were continually superfused with non-desensitizing concentrations of ACh (100–500 nM) while voltage-clamping at a holding potential of 0 mV to minimize the electrochemical gradient for Ca^{2+} entry, and were transiently pulsed to −120 mV to promote Ca^{2+} influx. To normalize for variability between oocytes, in each oocyte we express flash durations relative to that (flash strength of 1.0) required to just evoke puffs. IP_3-evoked Ca^{2+} signals were compared before and after applications of hyperpolarizing pulses to drive Ca^{2+} influx and thereby promote ER store filling. A 10-s delay was given between the end of the hyperpolarizing pulse and UV flash to allow cytosolic Ca^{2+} to return to basal levels, and intervals of 2 min were allowed between trials. Fig. 1*B* illustrates representative fluorescent profiles obtained in response to this protocol from a control oocyte (*upper*) and from an oocyte injected with the non-metabolizable cADPR analogue, 3-deaza-cADPR (*lower*) in response to photolysis flashes (relative flash strength 1.5) that evoked Ca^{2+} waves. In other experiments we examined the effects of cADPR in the same oocytes, leaving oocytes for 1 h after obtaining control records, and then injected them with 3-deaza-cADPR before repeating the protocol.

In control oocytes (not injected with 3-deaza-cADPR), elevations of cytosolic Ca^{2+} induced by 10 s hyperpolarizing pulses produced no significant change in global Ca^{2+} signals evoked by subsequent photorelease of IP_3 with normalized flash strengths of 1.5 or 2 (Figs. 1*B* and 2*A*, *left panel*). Subsequent injection of these oocytes with 3-deaza-cADPR also produced no significant change in amplitude of Ca^{2+} signals evoked by

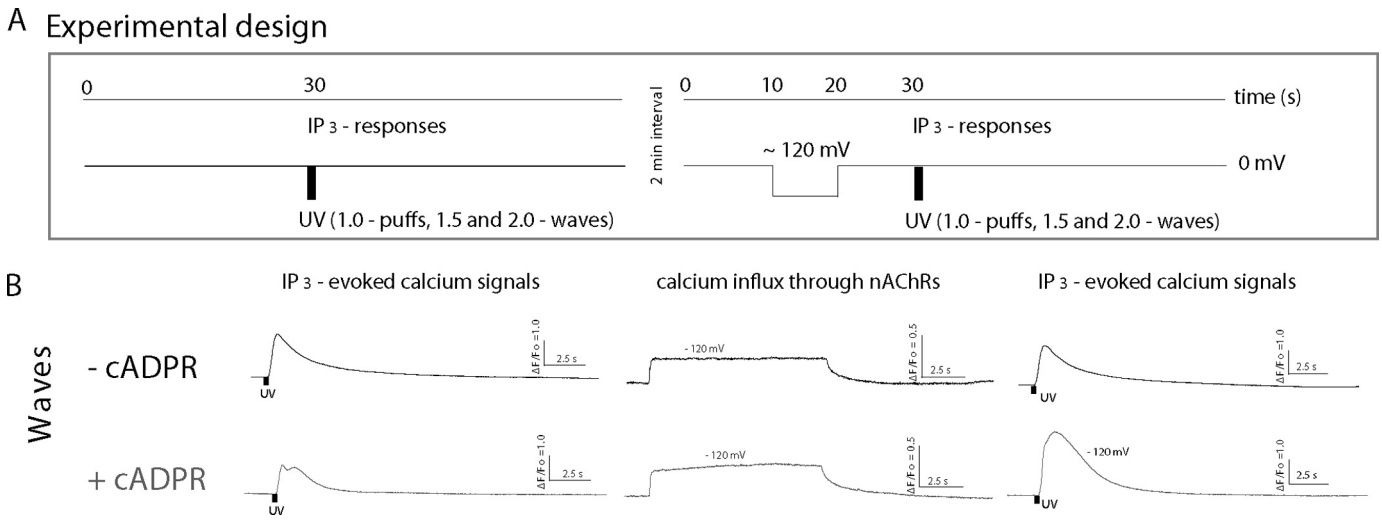

FIGURE 1. **Experimental protocol and representative examples of IP_3-evoked global Ca^{2+} signals before and after evoking Ca^{2+} influx.** *A*, schematic of the flash photolysis and voltage-clamp protocol. Oocytes were clamped at a holding potential of 0 mV, and IP_3 was photoreleased to evoke global Ca^{2+} waves (*left*). After a 2-min interval, a voltage pulse to −120 mV was applied for 10 s to drive Ca^{2+} influx through nAChR, followed 10 s later by a photolysis flash of the same strength (*right*). *B*, representative examples of fluorescence profiles of IP_3-evoked global Ca^{2+} responses, before (*left*) and after (*right*) Ca^{2+} influx, recorded in oocytes without (*top*) and with cADPR (*bottom*). Localization of puff events in the imaging field is mapped in sent panels. IP_3-evoked Ca^{2+} signal is greater after induction of Ca^{2+} influx in the presence of 3-deaza-cADPR. *Traces* in the middle show Ca^{2+} fluorescence recorded during the hyperpolarizing voltage pulses.

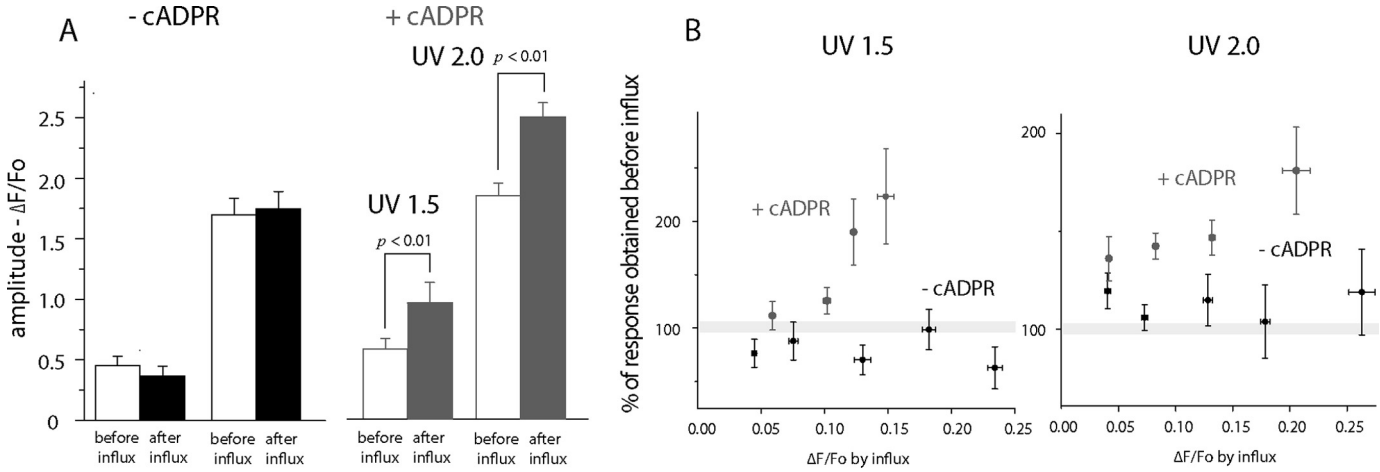

FIGURE 2. **IP_3-induced global Ca^{2+} signals are potentiated following Ca^{2+} influx in oocytes injected with 3-deaza-cADPR.** *A*, mean peak amplitudes of IP_3-induced global Ca^{2+} signals ($\Delta F/F_o$), evoked by UV flashes with normalized strengths of 1.5 and 2.0 in control (*left*) and 3-deaza-cADPR-injected oocytes (*right*). *Open bars* show measurements before Ca^{2+} influx, and *filled bars* are paired measurements from the same oocytes after influx. *B*, potentiation of IP_3-evoked signals as a function of magnitude of Ca^{2+} influx during the hyperpolarizing pulse. Measurements of IP_3-evoked responses on the ordinate are expressed as a percentage of the control value in each oocyte prior to the hyperpolarizing pulse. The abscissa shows plateau levels of fluorescence change ($\Delta F/F_o$) attained during the pulse, with data grouped into bins as indicated by horizontal error bars (+1 S.E.). Results are shown for two different UV photolysis flash strengths, without (*black symbols*) and with 3-deaza-cADPR (*red*). $n = 10$ oocytes, each examined before and after loading 3-deaza-cADPR, and 1 additional control oocyte. Data show mean $\Delta F/F_o \pm$ S.E. of measurements from between 4 and 10 regions of interest in each oocyte.

photorelease of IP_3 before Ca^{2+} influx (compare *open bars* ± cADPR in Fig. 2*A*). However, in marked contrast to controls, 3-deaza-cADPR-loaded oocytes displayed a strong potentiation of IP_3-evoked signals following Ca^{2+} influx (Figs. 1*B* and 2*A*, *right panel*). Those data were pooled from oocytes that showed varying amplitudes of hyperpolarization-induced Ca^{2+} elevation, likely as a result of varying expression levels of nAChR. In Fig. 2*B* we further show the percentage potentiation of IP_3-mediated signals evoked by the two flash strengths as a function of the fluorescence change ($\Delta F/F_0$) attained during the hyperpolarizing pulse. In the absence of 3-deaza-cADPR no appreciable potentiation was evident, even with cytosolic Ca^{2+} elevations giving fluorescence increases as great as $\Delta F/F_0$ 0.25. On the other hand, 3-deaza-cADPR-loaded oocytes showed a clear potentiation, which increased in a graded manner with increasing Ca^{2+} influx.

As considered further in the "Discussion," we interpret the enhancement of Ca^{2+} liberation through IP_3R as arising through enhanced ER Ca^{2+} store filling as a result of the combined effects of cADPR and elevated cytosolic [Ca^{2+}] to accelerate SERCA activity. Moreover, the lack of effect of either stimulus alone suggests that individually they neither appreciably promote store filling, nor act by other mechanisms to promote the opening of IP_3R channels.

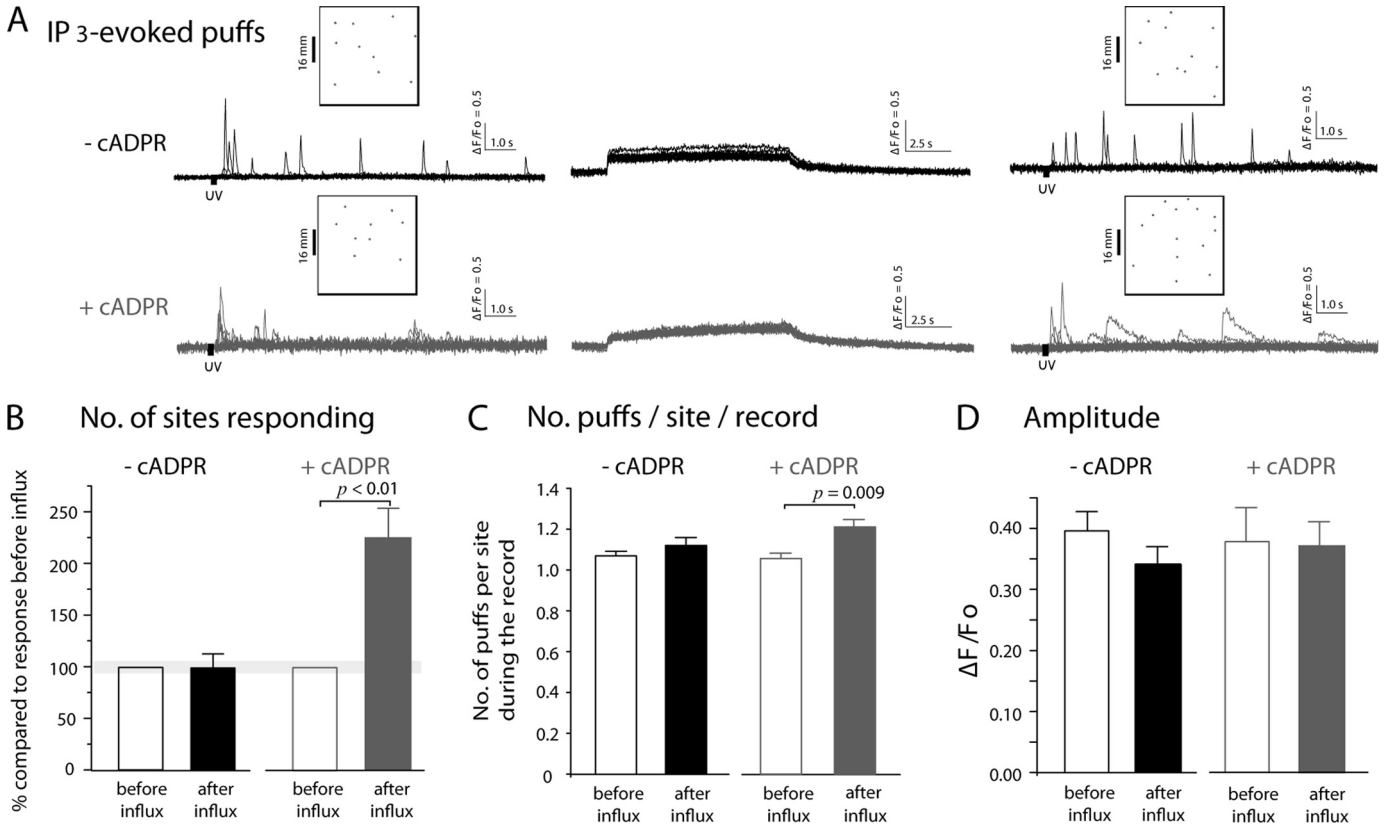

FIGURE 3. **Effects of prior Ca^{2+} influx on puffs in oocytes injected with 3-deaza-cADPR.** *A*, representative examples of local fluorescence signals showing puffs evoked before and after Ca^{2+} influx. Superimposed traces show recordings from 10 puff sites before influx and 11 sites after influx in control oocytes (*black*); and from 9 sites before influx and 14 sites after influx in oocytes injected with 3-deaza-cADPR (*gray*). *B*, following Ca^{2+} influx in oocytes injected with 3-deaza-cADPR the numbers of puff sites responding to photoreleased IP$_3$ were greatly increased. Data are normalized to the numbers of sites responding to photoreleased IP$_3$ in each oocyte before influx. *C*, mean numbers of puffs observed at each responding site during 35-s recordings following photolysis flashes. In oocytes lacking 3-deaza-cADPR, puff frequencies did not change after Ca^{2+} influx (before Ca^{2+} influx 1.07 ± 0.02 puffs per site and after 1.12 ± 0.04, $p < 0.05$). Oocytes injected with 3-deaza-cADPR exhibited a significant increase in frequency following Ca^{2+} influx (1.06 ± 0.02 puffs per site before influx, 1.21 ± 0.03 after influx, $p = 0.01$). *D*, mean amplitudes ($\Delta F/F_o$) of initial puffs observed at each responding site before and after Ca^{2+} influx in control and 3-deaza-cADPR-injected oocytes (before Ca^{2+} influx $\Delta F/F_o$ 0.39 ± 0.03, 116 puffs, after Ca^{2+} influx $\Delta F/F_o$ 0.34 ± 0.03, 126 puffs: oocytes injected with 3-deaza-cADPR; before Ca^{2+} influx $\Delta F/F_o$ 0.38 ± 0.06, 86 puffs, after Ca^{2+} influx, $\Delta F/F_o$ 0.37 ± 0.04, 176 puffs). There are no significant differences ($p > 0.05$). All data in this figure were obtained from 11 control oocytes and 10 oocytes injected with 3-deaza-cADPR, obtained from 5 frogs.

Effects of ER Store Filling on Local Ca^{2+} Puffs—IP$_3$-evoked puffs are the unitary events that serve as "building blocks" to initiate and propagate Ca^{2+} signals via Ca^{2+}-induced Ca^{2+} release (CICR), and result from the concerted opening of small numbers of IP$_3$R grouped within clusters (22–24). We thus analyzed the effects of cADPR on puffs to obtain more detailed mechanistic information on how increased luminal Ca^{2+} might affect IP$_3$R function at the level of these elementary Ca^{2+} signals. Puffs were evoked using shorter photolysis flashes (normalized flash strength = 1) than used to trigger waves, and oocytes were loaded with the slow Ca^{2+} buffer EGTA (final intracellular concentration ~300 μM) to inhibit cluster-cluster interactions and promote the balkanization of global Ca^{2+} waves into local signals (25).

Under these conditions, photorelease of IP$_3$ evoked puffs from several discrete sites within the 40 × 40 μm imaging field (Fig. 3*A*, *inset panels*). Recordings ($\Delta F/F_o$) were made from small (1.5 μm square) regions of interest centered on puff sites, and showed events with highly variable amplitudes arising after differing latencies (Fig. 3*A*). Measurements were obtained from control oocytes and oocytes injected with 3-deaza-cADPR; mean cytosolic Ca^{2+} elevations during hyperpolarizing pulses were closely similar between these groups (respective $\Delta F/F_o$ 0.22 ± 0.0 and 0.19 ± 0.02).

The most prominent effect in cADPR-loaded oocytes was a marked increase in the number of sites where puffs were observed following Ca^{2+} influx as compared with the number of responding sites before influx. Because the numbers of active puff sites increase as a steep function of [IP$_3$] (22), we corrected for variability between oocytes in loading of caged IP$_3$ and in flash strengths by expressing responses as a percentage of that obtained in each cell before Ca^{2+} influx. Ca^{2+} influx resulted in a greater than 2-fold potentiation in number of responding sites in oocytes injected with 3-deaza-cADPR (Fig. 3*B*; 223.7 ± 29.5%, whereas non-injected oocytes failed to show any significant change (98.7 ± 13.5%). Potentiation in the number of puff per site during the record was also observed in oocytes injected with 3-deaza-cADPR (Fig. 3*C*; control: 1.06 ± 0.02 puffs per site before Ca^{2+} influx, 1.12 ± 0.04 after Ca^{2+} influx, $p > 0.05$, 11 oocytes from five different batches 3-deaza-cADPR: 1.06 ± 0.02 before Ca^{2+} influx, 1.21 ± 0.03 after Ca^{2+} influx, p, 0.009). Notably, and in contrast to the effect on global Ca^{2+} signal amplitude, we did not detect significant changes in mean puff amplitudes under any condition (Fig. 3*D*).

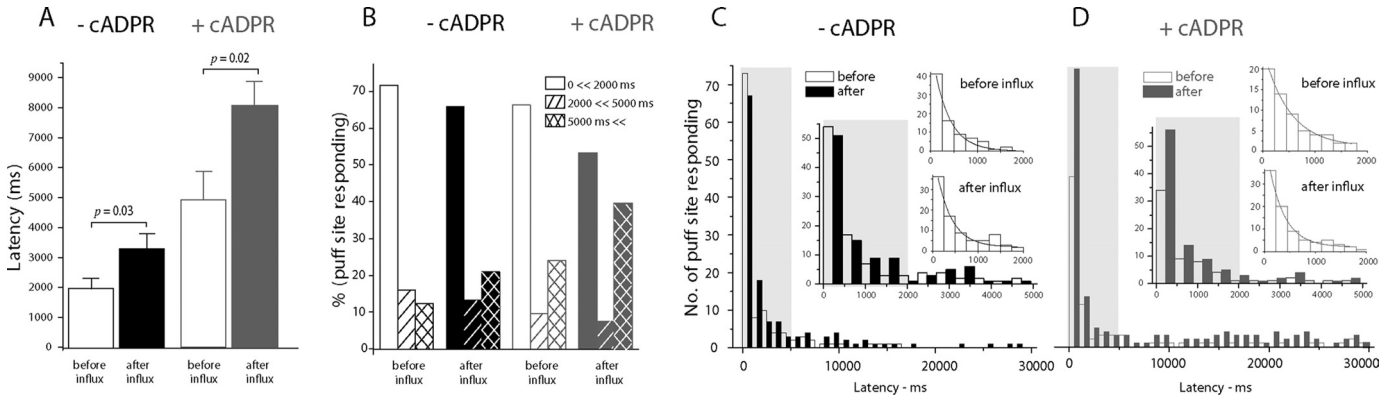

FIGURE 4. **Changes in first-puff latencies with Ca^{2+} influx and 3-deaza-cADPR.** Latencies were measured as the time from end of the photolysis flash to the observation of the first puff at any given site. *A*, mean values of latencies in control and 3-deaza-cADPR-injected oocytes before (*open bars*) and after (*filled bars*) Ca^{2+} influx. Paired measurements were made in each oocyte before and after Ca^{2+} influx and show significant differences for both experimental groups; but wide experimental variation between oocytes makes statistical comparison difficult between control and 3-deaza-cADPR groups. *B*, increases in mean puff latencies with Ca^{2+} influx and 3-deaza-cADPR largely arise from the appearance of long-latency puffs. Histograms show the proportion of initial puffs under each experimental condition that arose within <2s, 2–5s, and >5s following the photolysis flash. *C* and *D*, distributions of first-puff latencies before (*open bars*) and after Ca^{2+} influx (*filled bars*) in control (*C*) and 3-deaza-cADPR-injected oocytes (*D*). Data are plotted on 3 timescales to more clearly illustrate the relative invariance of the population of short latency (<2s) puffs, and the appearance of puffs with latencies of tens of seconds. Measurements were obtained from 11 control oocytes and 10 oocytes injected with 3-deaza-cADPR. Curves are single exponential fits to data at latencies <2s.

Store Filling Promotes a Population of Long Latency Puffs—Puff latencies (time from the end of UV flash to the first puff at a given site) provide a sensitive measure of IP_3R activation via cytosolic receptor sites, and shorten as a steep function of both increasing [IP_3] (22) and basal cytosolic [Ca^{2+}].[3] We were thus interested to examine whether puff latencies are further modulated by changes in ER Ca^{2+} loading induced by Ca^{2+} influx with or without concomitant injection of 3-deaza-cADPR (Fig. 4*A*). Unexpectedly, mean latencies were prolonged following Ca^{2+} influx in control oocytes (1961 ± 312 ms before Ca^{2+} influx $n = 116$; 3296 ± 489 ms after Ca^{2+} influx, $n = 126$, $p = 0.027$), and this prolongation was even more pronounced in oocytes injected with 3-deaza-cADPR (4923 ± 929 ms before Ca^{2+} influx, $n = 86$; 8046 ± 819 ms after Ca^{2+} influx, $n = 176$, $p = 0.019$). Moreover, mean latencies were longer comparing control and cADPR-injected oocytes both before and after Ca^{2+} influx.

The prolongation of puff latencies arose in all instances largely because of an increased proportion of initial puffs occurring after latencies of more than 5 s (Fig. 4*B*). This is analyzed in more detail in Fig. 4, *C* and *D*, showing the distributions of puff latencies on various timescales for the four experimental conditions. In all cases, the majorities of events arose within about 2 s of the photolysis flash, and distributed closely following a single exponential function. Time constants of exponential fits indicate that the latencies of these early puffs actually shortened following Ca^{2+} influx in the presence of 3-deaza-cADPR (control oocytes; before Ca^{2+} influx, 339 ± 35 ms, after Ca^{2+} influx, 336 ± 44 ms: oocytes injected with 3-deaza-cADPR; before Ca^{2+} influx, 497 ± 63 ms, after Ca^{2+} influx, 314 ± 20 ms). Instead, the prolongation of mean latencies is entirely attributable to the appearance of a population of puffs with latencies widely and non-exponentially distributed between about 5 s and 30 s. These delayed puffs were most prominent following Ca^{2+} influx in oocytes injected with 3-deaza-cADPR (Fig. 4, *B* and *D*), but were evident also in these oocytes before influx, and in control oocytes after influx (Fig. 4, *B* and *C*).

ER Store Filling Prolongs Puff Kinetics—In the course of these experiments we observed that a high proportion of puffs evoked after Ca^{2+} influx in oocytes injected with 3-deaza-cADPR displayed unusually slow kinetics (Fig. 5*A*). To quantify this effect, we measured puff durations as full duration at half-maximal fluorescence amplitude (FDHM). Puff durations in oocytes without 3-deaza-cADPR injection (7 oocytes from 3 frogs) showed no significant difference before and after Ca^{2+} influx (Fig. 5*B*: before Ca^{2+} influx FDHM = 105.7 ± 9.2 ms, $n = 72$ puffs; after Ca^{2+} influx 109.6 ± 13.6 ms, $n = 97$). Injection of 3-deaza-cADPR in the same oocytes resulted in a slightly longer mean FDHM before Ca^{2+} influx as compared with control oocytes. After Ca^{2+} influx, the mean FDHM in 3-deaza-cADPR injected oocytes became about 2-times longer after Ca^{2+} influx (Fig. 5*B*: before Ca^{2+} influx 125.0 ± 19.8 ms, $n = 62$; after Ca^{2+} influx, 264.7 ± 20.2 ms, $n = 132$). This effect is shown in more detail in Fig. 5, *C–F*, plotting distribution histograms of puff durations for each condition. In all cases, excepting puffs after Ca^{2+} influx in 3-deaza-cADPR-injected oocytes, the durations closely followed mono-modal, skewed distributions, with most events having durations (FDHM) around 50–100 ms and showing a roughly exponential fall-off in events with progressively longer durations (Fig. 5, *C–E*). Dramatically different from this, puffs evoked by photorelease of IP_3 after Ca^{2+} influx in the presence of 3-deaza-cADPR showed a bimodal distribution of durations, with about an equal proportion showing short durations as in the other conditions, and a new population with a mean duration around 500 ms (Fig. 5*F*).

Long Latency Puffs Have Prolonged Durations and Attenuated Amplitudes—It was apparent from visual inspection that those puffs with prolonged durations tended to occur with long latencies. This is illustrated in Fig. 6, showing scatter plots of puff latency *versus* puff duration for the four experimental conditions. Excepting for puffs arising after Ca^{2+} influx in the presence of 3-deaza-cADPR there were few events with durations

[3] M. Yamasaki-Mann and I. Parker, unpublished observations.

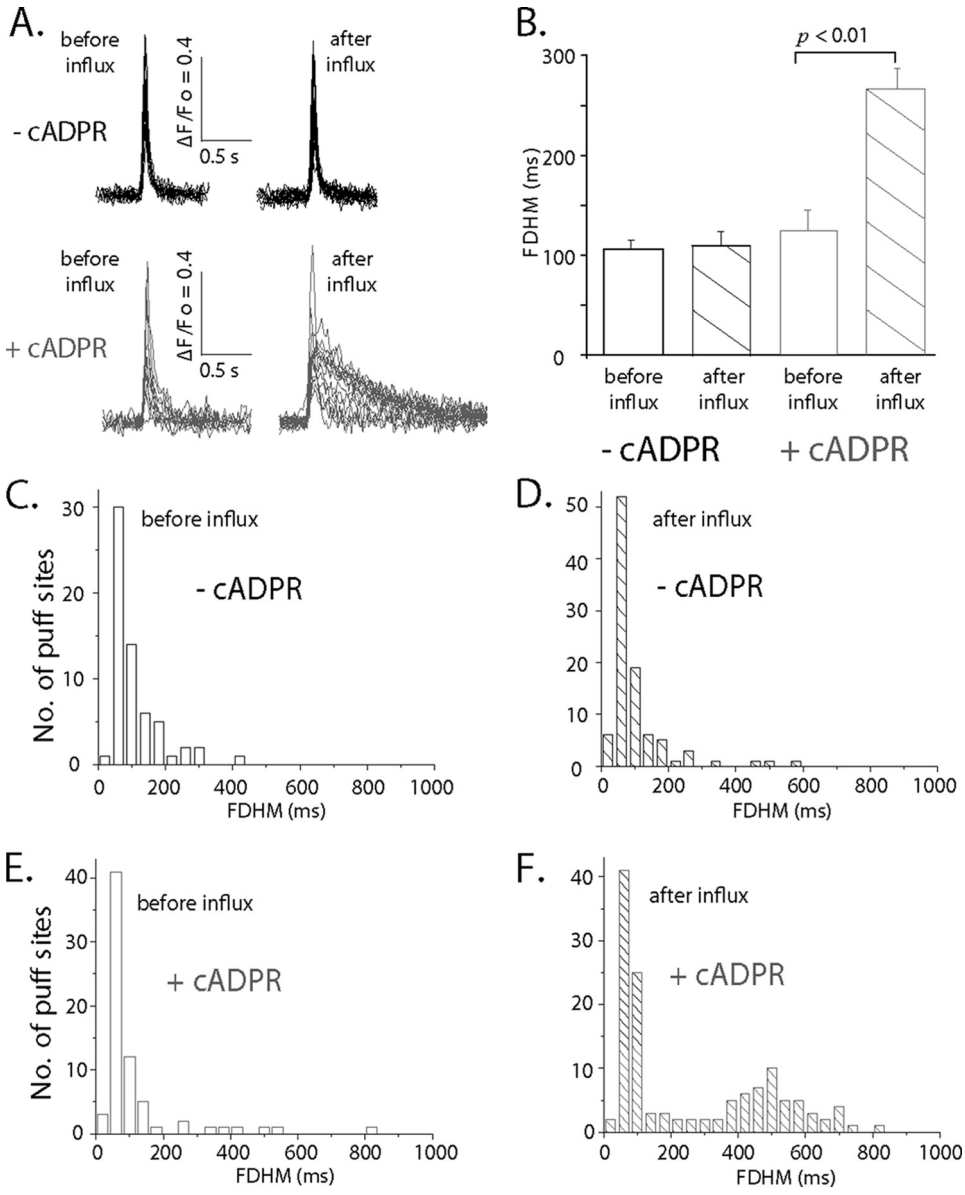

FIGURE 5. **Puff durations are prolonged after Ca^{2+} influx in 3-deaza-cADPR-injected oocytes.** *A*, superimposed traces illustrating representative examples of puffs evoked before (*left*) and after (*right*) Ca^{2+} influx before and after injection of 3-deaza-cADPR. *B*, puff durations, measured as full-duration at half-maximal (FDHM) fluorescence amplitude for each of the four experimental conditions. Data were obtained from 7 oocytes, from which paired measurements were obtained before and after loading 3-deaza-cADPR. *C–F*, histograms plotting distributions of first-puff latencies for each condition. Data are from 7 oocytes from 3 different frogs.

longer than 200ms, and the occurrence those prolonged puffs did not show any obvious correlation with latency (Fig. 6, *A–C*). On the other hand, puffs evoked after Ca^{2+} influx in the presence of 3-deaza-cADPR distributed as two clearly distinct populations (Fig. 6*D*); brief events arising mostly after short latencies, with a distribution on the scatter plot (circled as region 1) matching that of the other experimental conditions, and a new population of prolonged events, mostly arising after long latencies (region 2).

Puffs with prolonged durations tended to be smaller than short-duration puffs (*e.g. inset traces*, Fig. 6*D*). To quantify this effect we measured the amplitudes of puffs before and after Ca^{2+} influx in 3-deaza-cADPR-injected oocytes and grouped them according to their duration (FDHM <200 ms and >200 ms: Fig. 6, *E* and *F*, respectively). Consistent with the result in Fig. 3*D*, there was no significant difference in overall mean puff amplitudes before and after Ca^{2+} influx. However, puffs with shorter FDHM (<200 ms) exhibited larger amplitudes compared with those with the longer FDHM (>200 ms), an effect that became more prominent ($p < 0.001$) after Ca^{2+} influx (Fig. 6*F*).

To determine whether the prolonged, low amplitude puffs arise from the same sites that showed brief, larger events before Ca^{2+} influx or whether they involve recruitment of new sites, we searched for sites that gave puffs both before and after Ca^{2+} influx. In general puffs evoked after Ca^{2+} influx arose at sites different from those responding before influx (*e.g.* Fig. 3*A*, *inset panels*), and we were able to identify only 6 sites for paired measurements. Nevertheless, these showed significantly longer durations (mean duration after influx 202.3 ± 28.2% as compared with before influx, $p < 0.05$) and smaller amplitudes (76.2 ± 8.7%, $p < 0.05$).

DISCUSSION

Using *Xenopus* oocytes, which do not express RyRs, we had previously shown that a non-metabolizable analog of second messenger cADPR speeds the clearance of Ca^{2+} ions from the cytosol by accelerating SERCA pumping rate (17). Here, we demonstrate a potential physiological role for cADPR in modulating IP_3-mediated Ca^{2+} signals by a store-filling mechanism in *Xenopus* oocytes; and further investigate the ways in which local IP_3-evoked Ca^{2+} puffs are affected by changes in luminal ER Ca^{2+} level.

Several previous studies have investigated the actions of cADPR on Ca^{2+} release through ER channels (26–28), and have also implicated a role for cADPR in regulating ER Ca^{2+} store filling (29). However, interpretation of the results is confounded because the cell types employed express both RyRs and IP_3Rs. RyRs are modulated directly/indirectly by cADPR and by luminal [Ca^{2+}], and in light of their mutual interaction with IP_3Rs via CICR it is difficult to discern whether cADPR may act on IP_3R-mediated Ca^{2+} liberation independently of RyRs. We thus employed *Xenopus* oocytes as a model cell system that

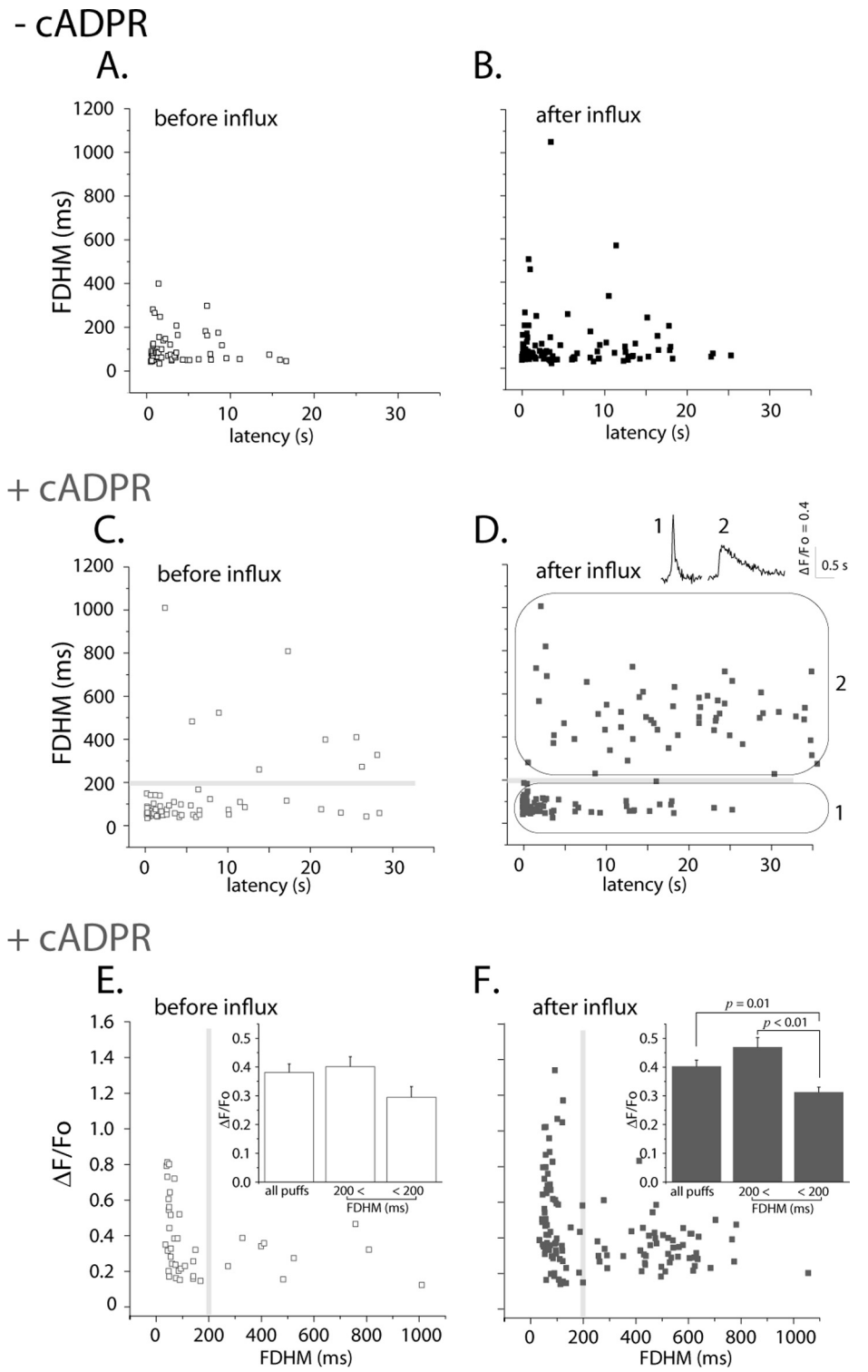

FIGURE 6. **Long latency puffs observed after Ca^{2+} influx in the presence of 3-deaza-cADPR also exhibit prolonged durations.** *A–D*, graphs show scatter plots of latencies of initial puffs *versus* their durations (FDHM) for each of the four experimental conditions. Ca^{2+} influx in 3-deaza-cADPR-injected oocytes resulted in the appearance of a population of long-latency, prolonged puffs (region marked as 2 in *D*), distinct from the population of short-latency, brief puffs (region 1) that was predominant in the other experimental conditions. *Insets* in *D* illustrate typical examples of puffs from these two populations. Data are from the same oocytes used for analysis in Fig. 5. *E* and *F*, scatter plots of durations (FDHM) of initial puffs *versus* their peak amplitudes, measured in cADPR-injected oocytes before and after Ca^{2+} influx, respectively. *Insets* present mean values for all puffs, puffs with FDHM <200 ms, and puffs with FDHM >200 ms. Respective puff amplitudes before influx were $\Delta F/F_o$ 0.38 ± 0.03 (pooling all 62 puffs), 0.40 ± 0.03 (53/72 puffs with FDHM < 200 ms) and 0.29 ± 0.03 (9/62 puffs 56/132 puffs with FDHM > 200 ms): and for puffs after influx 0.40 ± 0.02 (pooling al 132 puffs), 0.46 ± 0.03 (76/132 puffs with FDHM < 200 ms) and 0.31 ± 0.02 (56/132 puffs with FDHM > 200 ms).

lacks RyRs to study the actions of cADPR on Ca^{2+} signals evoked by photoreleased IP_3.

We observed a potentiation in the peak amplitude of IP_3-evoked global Ca^{2+} signals and in the numbers of responding puff sites following injection of 3-deaza-cADPR into oocytes, but only when tested after transient elevation of cytosolic [Ca^{2+}] induced by Ca^{2+} influx through expressed nAChR. In conjunction with our earlier findings (17), this strongly suggests that the potentiation arises through enhanced filling of ER luminal Ca^{2+} stores (12), and not through any putative direct cytosolic effects of cADPR on IP_3R. Most importantly, 3-deaza-cADPR had little or no effect on IP_3-induced signals under basal conditions of resting cytosolic [Ca^{2+}]. Moreover, transient elevations of cytosolic [Ca^{2+}] had little effect in the absence of cADPR loading. Although responses to IP_3 are highly sensitive to cytosolic Ca^{2+} levels at the time of stimulation (30, 31), we measured signals evoked by photoreleased IP_3 10 s after terminating Ca^{2+} influx, at a time when the Ca^{2+} fluorescence had returned to basal levels. Similarly, the lack of effect of Ca^{2+} influx in the absence of cADPR indicates that other potential interactions between cytosolic Ca^{2+} and IP_3R function, including stimulated production of IP_3 by phospholipase C (32), phosphorylation of the IP_3R by protein kinase A (33), or modulation of IP_3R function by enhanced ATP production (34), played no significant role. That result is also consistent with findings that basal SERCA activity in oocytes is low (17), so that the transient Ca^{2+} elevations we applied were insufficient to result in appreciable ER store filling in the absence of cADPR. Finally, we note that we were able to mimic the effects of cADPR on puffs by overexpressing SERCA2b to enhance Ca^{2+} uptake into the ER (21). In comparison to control oocytes (without SERCA 2b overexpression) the numbers of puffs evoked per site following Ca^{2+} influx increased by

78%, and the amplitudes, durations (FDHM) and latencies of the initial puffs at each site were, respectively 38, 36, and 360% greater.

The finding that cADPR in conjunction with Ca^{2+} influx resulted in the appearance of puffs that arise after long latencies and show prolonged durations was unexpected and intriguing. These long and delayed events appear to form a kinetically distinct population from the normal brief, short latency puffs (Fig. 6*D*). However, we did observe some instances where a given puff site showed a normal puff before Ca^{2+} influx and a delayed and prolonged puff after influx suggesting that the prolonged puffs do not arise through activation of previously silent sites, but rather that the properties of IP_3R at a site may be altered by elevated luminal [Ca^{2+}]. How then might this arise? One potential mechanism is mediation via cytosolic Ca^{2+} regulatory sites on the IP_3R. An increased luminal [Ca^{2+}] is expected to cause a greater instantaneous Ca^{2+} flux (current) through open IP_3R channels which, even though it may not be readily manifest in macroscopic fluorescence puff signals, would result in higher local Ca^{2+} concentrations in the immediate vicinity of receptor sites on that and closely adjacent IP_3Rs. It is, however, difficult to envision how such a mechanism could prolong puff latencies. Rather, increased Ca^{2+} flux through stochastic openings of single IP_3R channels might increase the probability of opening of neighboring channels to trigger puffs with shorter latencies (35). Alternatively, several studies describe modulation of IP_3R function by luminal Ca^{2+}, acting either directly on the receptor protein (14, 36) or via luminal Ca^{2+}-binding proteins that regulate the IP_3R (15) (37). In addition, there is considerable evidence for heterogeneous distributions of SERCA pumps, IP_3R channels and luminal Ca^{2+}-binding proteins (38–42) so that spatial differences in luminal [Ca^{2+}] may differentially affect different puff sites; perhaps explaining the heterogeneous occurrence of both brief and prolonged puffs following Ca^{2+} influx.

In contrast to the potentiation in amplitude of global Ca^{2+} signals by the combined actions of cADPR and Ca^{2+} influx, the overall amplitude of local Ca^{2+} puffs was little changed, even though the numbers of responding puff sites increased substantially and puff durations became longer. The potentiation of global signals may therefore largely arise through the latter two effects on the underlying elementary release events. At first sight it is surprising that mean puff amplitudes remained constant (Fig. 3*D*), as increased luminal [Ca^{2+}] is expected to increase single-channel IP_3R Ca^{2+} flux. However, this result mirrors findings that puff amplitudes are remarkably insensitive to other factors, including [IP_3] (43, 44), even though they strongly affect puff frequencies and would also be expected to affect puff amplitudes by increasing the numbers of IP_3R channels that open within clusters. Smith & Parker (45) speculated that puff amplitudes may instead be regulated by feedback Ca^{2+} inhibition so as to maintain a roughly constant mean amplitude, and such a mechanism may apply also here. This conclusion is further supported by a more detailed analysis of puffs evoked following Ca^{2+} influx. Those puffs showing normal brief durations had mean amplitudes greater than puffs evoked before influx (Fig. 6*F*), consistent with an increased single-channel Ca^{2+} current. On the other hand, the prolonged puffs showed reduced amplitudes, suggesting that changes in IP_3R properties associated with increased ER Ca^{2+} store filling led to changes in both gating kinetics and aggregate Ca^{2+} flux through channels at a puff site. The mechanism underlying this behavior remains to be elucidated.

IP_3 and Ca^{2+} are together considered to constitute a cellular coincidence detector, because activation of IP_3R channels simultaneously requires both of these second messengers (1). We would now add cADPR as a further messenger that plays into this signaling mechanism, though acting on a different timescale. Specifically, acceleration of SERCA activity by cADPR promotes filling of ER stores when cytosolic Ca^{2+} is elevated prior to activation of the IP_3 pathway, providing an anticipatory signal that will likely persist for seconds or longer depending upon rates of cADPR catabolism and ER Ca^{2+} leakage. Indeed, the state of ER Ca^{2+} filling has been shown to powerfully affect intracellular Ca^{2+} signaling (46). Our results indicate that this mechanism is not necessarily constrained by a passive balance between rates of sequestration and release, and strengthen the notion that the versatility of Ca^{2+} signaling may be enhanced not only by modulation of release channels properties from the cytosolic side, but also from luminal side of the ER through messenger pathways that modulate Ca^{2+} sequestration mechanisms such as SERCA. In that regard, cADPR may be unique in playing multiple roles to directly regulate Ca^{2+} release through the RyR, accelerate cytosolic Ca^{2+} uptake by SERCA, and indirectly modulate both global IP_3-mediated responses and the local Ca^{2+} transients that signal to neighboring organelles such as mitochondria (47, 48).

Acknowledgment—We thank Andrew C. Charles (UCLA) for his insightful comments on this manuscript.

REFERENCES

1. Berridge, M. J., Bootman, M. D., and Roderick, H. L. (2003) *Nat. Rev. Mol. Cell Biol.* **4,** 517–529
2. Camacho, P., and Lechleiter, J. D. (1993) *Science* **260,** 226–229
3. Albrecht, M. A., Colegrove, S. L., and Friel, D. D. (2002) *J. Gen. Physiol.* **119,** 211–233
4. Yano, K., Petersen, O. H., and Tepikin, A. V. (2004) *Biochem. J.* **383,** 353–360
5. Friel, D. (2004) *Biol. Res.* **37,** 665–674
6. Bers, D. M., and Berlin, J. R. (1995) *Am. J. Physiol.* **268,** C271–C277
7. Györke, I., Hester, N., Jones, L. R., and Györke, S. (2004) *Biophys. J.* **86,** 2121–2128
8. Ching, L. L., Williams, A. J., and Sitsapesan, R. (2000) *Circ. Res.* **87,** 201–206
9. Sitsapesan, R., and Williams, A. J. (1995) *J. Membr. Biol.* **146,** 133–144
10. Missiaen, L., Taylor, C. W., and Berridge, M. J. (1991) *Nature* **352,** 241–244
11. Missiaen, L., De Smedt, H., Droogmans, G., and Casteels, R. (1992) *J. Biol. Chem.* **267,** 22961–22966
12. Parys, J. B., Missiaen, L., De Smedt, H., and Casteels, R. (1993) *J. Biol. Chem.* **268,** 25206–25212
13. Oldershaw, K. A., and Taylor, C. W. (1993) *Biochem. J.* **292,** 631–633
14. Sienaert, I., Missiaen, L., De Smedt, H., Parys, J. B., Sipma, H., and Casteels, R. (1997) *J. Biol. Chem.* **272,** 25899–25906
15. Higo, T., Hattori, M., Nakamura, T., Natsume, T., Michikawa, T., and Mikoshiba, K. (2005) *Cell* **120,** 85–98
16. Parys, J. B., Sernett, S. W., DeLisle, S., Snyder, P. M., Welsh, M. J., and Campbell, K. P. (1992) *J. Biol. Chem.* **267,** 18776–18782

17. Yamasaki-Mann, M., Demuro, A., and Parker, I. (2009) *Cell Calcium* **45,** 293–299
18. Galione, A., Lee, H. C., and Busa, W. B. (1991) *Science* **253,** 1143–1146
19. Guse, A. H. (2000) *J. Mol. Med.* **78,** 26–35
20. Demuro, A., and Parker, I. (2005) *J. Biomed. Opt.* **10,** 11002
21. Green, K. N., Demuro, A., Akbari, Y., Hitt, B. D., Smith, I. F., Parker, I., and Laferla, F. M. (2008) *J. Cell Biol.* **181,** 1107–1116
22. Yao, Y., Choi, J., and Parker, I. (1995) *J. Physiol.* **482,** 533–553
23. Callamaras, N., Marchant, J. S., Sun, X. P., and Parker, I. (1998) *J. Physiol.* **509,** 81–91
24. Marchant, J. S., and Parker, I. (2001) *EMBO J.* **20,** 65–76
25. Dargan, S. L., and Parker, I. (2003) *J. Physiol.* **553,** 775–788
26. Bruzzone, S., Kunerth, S., Zocchi, E., De Flora, A., and Guse, A. H. (2003) *J. Cell Biol.* **163,** 837–845
27. Morgan, A. J., and Galione, A. (2002) in *Cyclic ADP-Ribose and NAADP. Structures, Metabolism and Functions* (Lee, H. C., ed) Kluwer, Dordrecht
28. Cancela, J. M., Van Coppenolle, F., Galione, A., Tepikin, A. V., and Petersen, O. H. (2002) *EMBO J.* **21,** 909–919
29. Lukyanenko, V., Györke, I., Wiesner, T. F., and Györke, S. (2001) *Circ. Res.* **89,** 614–622
30. Taylor, C. W., and Laude, A. J. (2002) *Cell Calcium* **32,** 321–334
31. Swatton, J. E., and Taylor, C. W. (2002) *J. Biol. Chem.* **277,** 17571–17579
32. Várnai, P., and Balla, T. (1998) *J. Cell Biol.* **143,** 501–510
33. Wagner, L. E., 2nd, Joseph, S. K., and Yule, D. I. (2008) *J. Physiol.* **586,** 3577–3596
34. Betzenhauser, M. J., Wagner, L. E., 2nd, Iwai, M., Michikawa, T., Mikoshiba, K., and Yule, D. I. (2008) *J. Biol. Chem.* **283,** 21579–21587
35. Shuai, J., Pearson, J. E., Foskett, J. K., Mak, D. O., and Parker, I. (2007) *Biophys. J.* **93,** 1151–1162
36. Horne, J. H., and Meyer, T. (1995) *Biochemistry* **34,** 12738–12746
37. Thrower, E. C., Choe, C. U., So, S. H., Jeon, S. H., Ehrlich, B. E., and Yoo, S. H. (2003) *J. Biol. Chem.* **278,** 49699–49706
38. Petersen, O. H., Tepikin, A., and Park, M. K. (2001) *Trends Neurosci.* **24,** 271–276
39. Hirose, K., and Iino, M. (1994) *Nature* **372,** 791–794
40. Pozzo-Miller, L. D., Connor, J. A., and Andrews, S. B. (2000) *J. Physiol.* **525,** 53–61
41. Subramanian, K., and Meyer, T. (1997) *Cell* **89,** 963–971
42. Meldolesi, J., and Pozzan, T. (1998) *Trends Biochem. Sci.* **23,** 10–14
43. Rose, H. J., Dargan, S., Shuai, J., and Parker, I. (2006) *Biophys. J.* **91,** 4024–4032
44. Smith, I. F., Wiltgen, S. M., and Parker, I. (2009) *Cell Calcium* **45,** 65–76
45. Smith, I. F., and Parker, I. (2009) *Proc. Natl. Acad. Sci. U.S.A.* **106,** 6404–6409
46. Patterson, M., Sneyd, J., and Friel, D. D. (2007) *J. Gen. Physiol.* **129,** 29–56
47. Rizzuto, R., Marchi, S., Bonora, M., Aguiari, P., Bononi, A., De Stefani, D., Giorgi, C., Leo, S., Rimessi, A., Siviero, R., Zecchini, E., and Pinton, P. (2009) *Biochim. Biophys. Acta* **1787,** 1342–1351
48. Olson, M. L., Chalmers, S., and McCarron, J. G. (2010) *J. Biol. Chem.* **285,** 2040–2050